

Elastic components for prosthetic skin

Stéphanie P. Lacour, *Member IEEE*, Ingrid Graz, Darryl Cotton, Siegfried Bauer, *Senior Member IEEE*, Sigurd Wagner, *Fellow IEEE*

Abstract—We have developed two fundamental components to manufacture a prosthetic skin: a stretchable pressure sensor formed of piezoelectric elastomer/ferroelectret multilayer sandwiched between stretchable electrodes and stretchable thin-film transistors. The components are prepared and embedded in silicone rubber, a polymer, which mimics the mechanical compliance of human skin. We demonstrate the stretchability of the sensory unit. In both relaxed and stretched states, the soft sensor skin transduces kPa pressures into electrical currents in the μA range.

I. INTRODUCTION

Over the last 5 years, considerable efforts have been spent in developing integrated prosthetic limbs that can restore significant motor functions of the natural limb [1-3]. A complex, associated challenge is to produce prosthetic limbs that would “feel” like the natural limb. One way to do this is to manufacture a compliant artificial skin, which will cover the prosthetic limb, provide sensory information and re-establish connections with the nervous system of the patient.

Biological skin has no equivalent in the world of today’s electronics. Integrated circuits and transducers provide high-level sensing and computation but do not stretch nor conform to the human body. Extensive research is being conducted to develop chronic therapeutic neural implants using microelectronics fabrication tools [4] but only few designs have reached the clinic.

The ideal prosthetic skin should look and sense like human skin; it wraps every contour of a bionic limb, moves in tandem with it, and ultimately interfaces with the nervous system. The task is colossal and requires finding materials, designs, fabrication and integration processes, which will enable high level of computing, (bio)mechanical compliance and biocompatibility.

An opportunity is rising with the development of so-called stretchable electronic circuits [5-8]. The circuits respond electrically like conventional electronics but behave

mechanically similarly to a rubber band, and can conform complex three-dimensional structures. Their technology relies on the integration of fragile electronic device materials and ultra-compliant polymers i.e. elastomers. Interestingly, similar technology is starting to be implemented to fabricate neural electrode implants [9].

In this paper, we focus on an elementary unit of the prosthetic skin: the sensory unit can sense pressure, and transduce the signal into a current pulse that would be capable of initiating an action potential in a single or a group of neurons. The elementary unit requires (i) a compliant electroactive material that provides the transducing function, (ii) an active electronic device that generates current, (iii) skin-like stretchable interconnects, which link the components together, and (iv) a biocompatible neural electrode interface. We have developed the first three components. We present their electrical, and detail their fabrication and electromechanical response.

II. DESIGN OF THE ARTIFICIAL SENSORY UNIT

In the human skin, touch is encoded and processed in four steps: reception, transduction, transmission and integration. A mechanoreceptor absorbs the energy of the physical stimulus and converts it into (electrical) membrane potential. Then the associated information (action potential) travels along the neuron’s axon to the central nervous system, which in turns decodes the frequency of the receptor signal.

Figure 1 proposes a schematic view of the prosthetic sensor unit: it consists of a wearable sensor circuit and an electrode implant. The soft sensor can detect applied pressure on the artificial skin and converts it in an electrical signal. Using a thin film transistor, the sensor output is further converted into an μA current, which could then be applied extracellularly to one or a few sensory fibers hosted in the nerve implant and initiate action potentials.

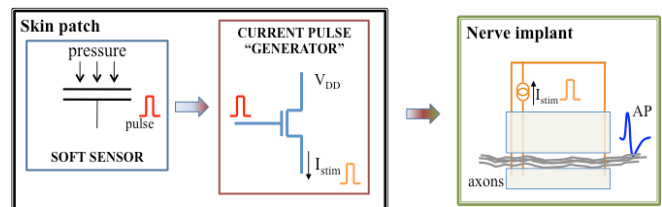


Fig. 1 Electrical model of the sensory unit for prosthetic skin. The skin patch is to be worn on the surface of the prosthetic limb; the neural implant is interfacing the sectioned peripheral nerve.

We have developed the components for the skin patch

Manuscript received April 15, 2011. This work was supported in part by the EPSRC Grant EP/C52330X/1, the Royal Society, and the ERC Starting Grant 259419.

S.P. Lacour was with the University of Cambridge, Cambridge UK. She is now with the Laboratory for Soft Bioelectronic Interfaces, Ecole Polytechnique Fédérale de Lausanne EPFL, Lausanne, Switzerland. (phone: +41-21-693-1181; e-mail: stephanie.lacour@epfl.ch).

I. Graz and S. Bauer are with the Johannes Kepler University, Linz, Austria. (e-mail: Ingrid.graz@jku.at, siegfried.bauer@jku.edu).

D. Cotton was with the University of Cambridge UK. He is now with Nokia, Cambridge UK (email: Darryl.cotton@nokia.com).

S. Wagner is with Princeton University, Princeton NJ, USA (email: wagner@princeton.edu).

with elastomeric materials, thin films and microfabrication tools.

The nerve implant is under development. Details on its current design can be found in [9-11]. Briefly, the implant is designed to interface a sectioned peripheral nerve and consists of an array of parallel microchannel hosting microelectrode arrays. Using asymmetric tripolar electrode configuration as illustrated Fig. 1, we can generate unidirectionally propagating action potentials thus ensure the artificial sensory signals will be transmitted to the central nervous system.

A. Soft pressure sensor

We prepare a highly compliant piezoelectric sensor by embedding $4 \times 4 \text{ mm}^2$ ferroelectret foils in a PDMS silicone matrix preliminary textured on the top and bottom faces.

Cellular HS06 polypropylene foams of 330 kg/m^3 density, $\sim 1 \text{ MPa}$ elastic modulus, and 1.3 relative permittivity are functionalized by corona discharge ($\sim 10 \text{ kV}$) to serve as piezoelectric-like ferroelectrets. Each foil exhibits a maximum longitudinal piezoelectric coefficient d_{33} of $\sim 200 \text{ pC/N}$. Ten ferroelectret sheets are stacked together using very thin PDMS layers as an interlayer adhesive. During the stacking, the positively-charged faces of the two neighboring ferroelectret sheets face each other, resulting in alternating positive/negative charged layers. After stacking, the multilayered ferroelectrets are cut into pieces of $4 \times 4 \text{ mm}^2$ surface area and $\sim 850 \mu\text{m}$ thickness.

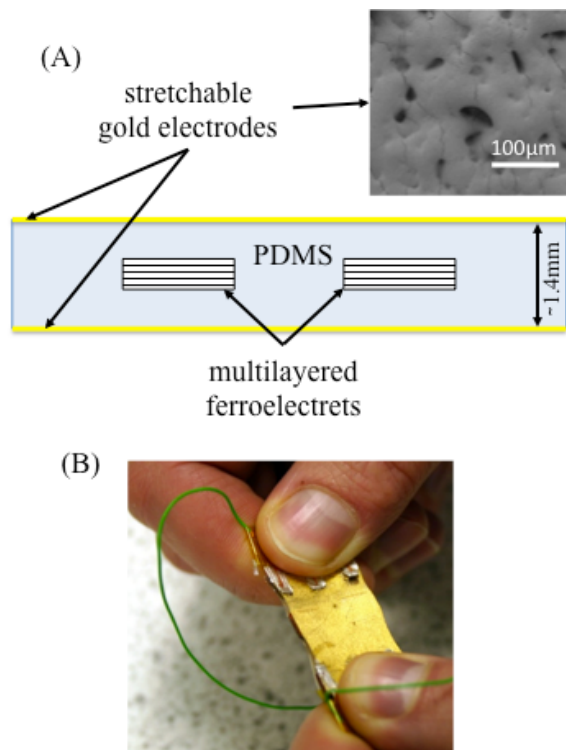


Fig. 2. Soft piezoelectric sensor. (A) Schematic cross-section of the elastomer/ferroelectret sensor and scanning electron micrograph of the macrotextured gold electrodes. (B) Picture of a device with 2×2 embedded multilayered ferroelectrets.

The ferroelectret multilayers are then embedded between two membranes of PDMS (Sylgard 184 Dow Corning, 20:1 weight ratio) (Fig. 2a). The outer side of each PDMS membrane is rough as the membranes are cast against 600 grit sandpaper. The resulting elastomer-ferroelectret-elastomer stack is about 1.4 mm thick and $50 \text{ mm} \times 20 \text{ mm}$ long and wide. Chromium/gold electrodes ($5 \text{ nm}/75 \text{ nm}$ thick) are subsequently evaporated on both (macrotextured) sides of the PDMS to form resilient stretchable electrodes (Fig. 2).

The piezoelectric soft sensor is then capacitively coupled to the gate electrode of the thin-film transistor TFT to complete the skin patch.

B. Current pulse “generator”

Thin film transistors (TFTs) can be fabricated directly on PDMS: they perform electrically well with electrical characteristics similar to those of their counterparts deposited on plastic foil. However TFTs patterned on uniform PDMS do not withstand mechanical deformation; the brittle TFT stack fractures upon mild bending ($< 1\%$ applied strain) and fails electrically.

We have optimized the mechanical design of TFTs on PDMS by engineering a gradient of stiffness in the elastomeric membrane itself. The TFTs are prepared on the stiffest region of the elastomer substrate and the metallic interconnects run across the substrate from stiff to soft to stiff, etc. regions. This ensures that upon large, applied macroscopic strain, the resulting strain in the stiffest TFT region remains close to zero and the strain gradient across the soft to stiff regions is low. Figure 3 shows a schematic cross-section of a stretchable TFT.

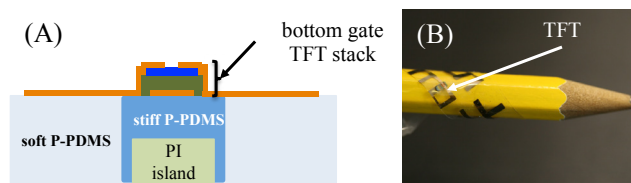


Fig. 3. Thin film transistor on silicone rubber. (A) Schematic cross-section of the device microfabricated on an elastomeric substrate with built-in strain relief. (B) Picture of an array of TFTs on 0.1 mm thick silicone membrane wrapped around a pencil. PI stand for polyimide, P-PDMS for photopatternable PDMS. The PI island is 2 mm diameter and $50 \mu\text{m}$ thick.

We adjust the compliance of the silicone membrane by locally controlling the elastomer's cross-linker density using UV lithography and photo-inhibiting benzophenone molecules [12]. Ratios in equivalent elastic modulus of up to 5 within have been demonstrated a single silicone membrane. Furthermore, increased mechanical contrast can be obtained by embedding stiffer polymer platforms e.g. polyimide or SU8 in the photo-patternable silicone matrix (P-PDMS). We have integrated such engineered soft substrates with pentacene TFTs and elastic thin gold film interconnects. The TFT process flow is described Fig. 4. First a polyimide island is embedded in a $100 \mu\text{m}$ thick spin-coated P-PDMS layer. Then the P-PDMS is UV exposed in a non-contact mode to UV light through a negative mask to

define the 2.4mm diameter “stiff” regions in the membrane (Fig. 4B).

After curing of the graded elastomer membrane, the bottom gate TFT stack is prepared with the following sequence: an evaporated chromium/gold (5nm/30nm) film gate electrode, a parylene C dielectric layer (600nm thick), an evaporated pentacene film (50nm thick) and 30nm thick gold film source and drain contacts. Each layer is patterned by shadow-masking [13]. The elastic moduli of the stiff and soft P-PDMS regions are 2.88MPa and 1.35MPa, respectively (that of the PI island is 3GPa).

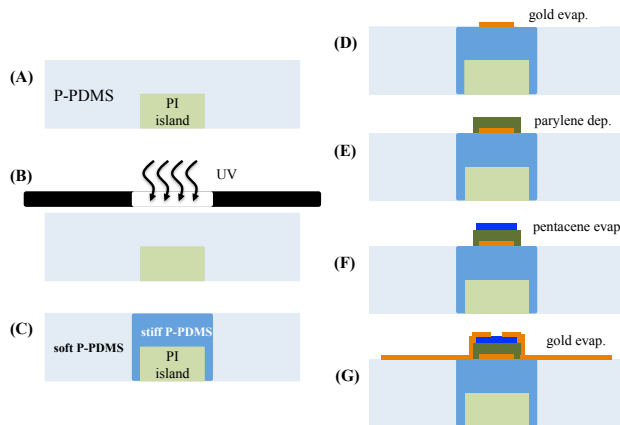


Fig. 4. Process flow to prepare a stretchable pentacene TFT on mechanically graded silicone membrane. (A). Encapsulation of the PI island in P-PDMS. (B). UV photolithography. (C). Curing of the membrane at 60°C overnight. (D). Evaporation of the gate electrode. (E). Deposition of the parylene dielectric. (F). Evaporation of the pentacene. (G). Evaporation of the source and drain electrodes.

III. RESULTS

A. Stretchable pentacene TFTs

Pentacene TFTs with 200 μ m wide and 100 μ m long channel patterned on engineered PDMS are characterized in a nitrogen controlled environment. The silicone membrane is mounted in a manual uni-axial stretcher. The transfer curves of a TFT held in the stretcher at different strains are presented

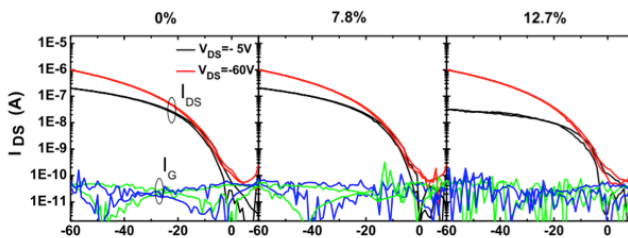


Fig. 5. Transfer curves of a stretchable pentacene TFT on engineered PDMS substrate recorded during a uni-axial stretch cycle to 7.8% and 12.7% strains. The TFT channel is 200 μ m wide and 100 μ m long.

When no strain is applied, the TFT operates reliably in the -60V to 0V range. Low leakage current is observed ($I_{gs} \sim 6$

$\times 10^{-11}$ A); the saturation mobility μ_{sat} is 0.105 cm²/V s, the on-off ratio is 8.6×10^3 , and the threshold voltage V_t is -5V. Upon uni-axial stretching, the electrical response of the pentacene TFT is stable. At 12.7% applied strain, the saturation mobility and the threshold voltage of the device are unchanged. After release of the strain, the performance of the TFT remains unchanged.

The TFT on mechanically graded silicone rubber is robust to large, macroscopic strain cycles.

B. Stretchable pressure sensor unit

Because the fabrication processes of the soft sensor and the stretchable TFT are not yet compatible, we have characterized the compliant “pressure to current” sensory unit in a hybrid configuration. The soft sensor is interfaced with an amorphous silicon TFT prepared on polyimide foil and laminated on the surface of the gold electrode. The description of the fabrication of the TFTs on polyimide can be found in [14].

The TFT operating point is set by applying a DC voltage V_{GS} to the gate (Fig. 6A). When a pressure is applied to the sensor element, the generated voltage directly modulates the conductance between the source and the drain contacts of the transistor. The hybrid pressure sensor circuit response is recorded when the sensor is stimulated with a cyclic pressure of 255kPa amplitude. With a bias voltage of +6V applied to the gate via $R_G = 1G\Omega$, and a drain source voltage of +10V, the generated voltage exceeds the threshold voltage of the TFT, and a drain-source current modulation of 1 μ A is recorded at a peak to peak pressure level of 255kPa (Fig. 6B, top). The drain-current is measured via a source follower circuit with a $R_L = 50\Omega$.

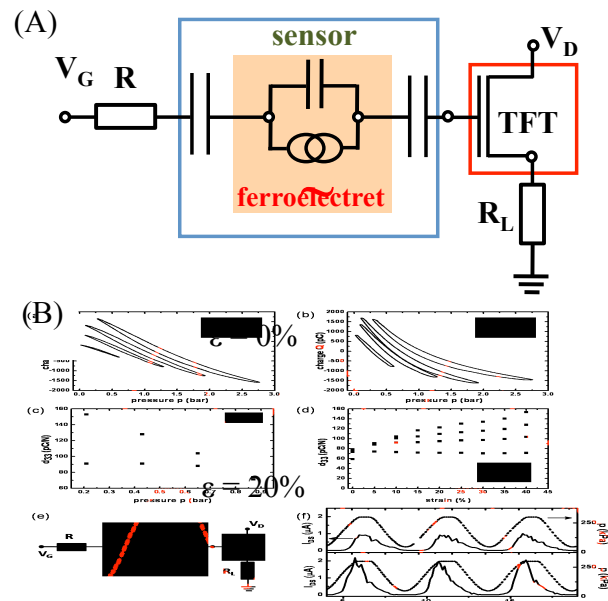


Fig. 6. Modulation of the source-drain current of the amorphous silicon thin film transistor when a 255kPa, 0.2Hz pressure wave is applied on the sensor surface, and when the soft sensory circuit is relaxed ($\epsilon = 0\%$) and uni-axially stretched ($\epsilon = 20\%$). Note that the apparent saturation in the applied pressure is due to an artefact in the measurement set-up.

When the applied pressure is small ($p < 50\text{kPa}$), the voltage on the TFT gate is not high enough to turn on the transistor and $I_{ds} \sim 0\text{A}$. Once the transistor turns on, the current quickly increases with the applied pressure to reach I_{max} at p_{max} . Then when the pressure decreases, I_{ds} slowly falls back to 0A . The $I_{ds}(t)$ profile is asymmetric because the charges generated across the ferroelectret stack leak quickly through the electrical leads preventing for a controlled modulation of I_{ds} decrease.

The same experiment is performed when the sensor is held stretched at $\epsilon = 20\%$. Fig. 6B (bottom) depicts the corresponding drain-source current. I_{ds} has increased to $I_{max} \sim 2\mu\text{A}$, further illustrating the enhanced piezoelectric response of the elastomer/ferroelectret sensor at large strain ($\epsilon \geq 20\%$). The stretchable pressure sensor skin was mechanically stretched and pressed more than twenty times, and no failure or signal degradation was observed.

In summary, we have demonstrated a stretchable pressure sensing electronic skin, which exhibits good pressure sensitivity and high stretchability that is similar to that of human skin. The stretchable elastomer-ferroelectret sensor unit cell provides the first example of a stretchable piezoelectric hybrid element. It is lightweight, fully elastic, highly sensitive, and does not require an external power supply. Further work is now required to integrate within a single silicone membrane the soft sensor and the TFT, and then distribute the elementary sensory unit into an array across a large-area skin patch. The sensitivity of the sensor and the sensor-TFT coupling should also be optimized so that smaller pressures (covering the physiological range of detectable stimulus) can reliably switch on the TFT.

REFERENCES

- [1] www.touchbionics.com
- [2] H. Ehrsson, B. Rosén, A. Stocksélius, C. Ragnö, P. Köhler, G. Lundborg, "Upper limb amputees can be induced to experience a rubber hand as their own," *Brain* vol. 131, 2008, pp. 2443-3452
- [3] P. D. Marasco, K. Kim, J.E. Colgate, M.A. Peshkin, T.A. Kuiken, "Robotic touch shifts perception of embodiment to a prosthesis in targeted reinnervation amputees", *Brain*, vol. 134, 2011, pp.747-758.
- [4] K.W. Horch, G.S. Dhillon, *Neuroprosthetics – Theory and Practice*. River Edge, NJ: World Scientific, 2004.
- [5] S. P. Lacour, J. Jones, S. Wagner, "Stretchable interconnects for elastic electronic surfaces," *Proceedings of the IEEE*, vol. 93, 2005, pp. 1459-1467
- [6] J. A. Rogers, T. Someya, and Y. Huang, "Materials and mechanics for stretchable electronics", *Science* vol. 327, 2010, pp. 1603-1607.
- [7] Stefan C. B. Mannsfeld, B.C-K. Tee, R.M. Stoltenberg, C.V. H-H. Chen, S. Barman, B.V.O. Muir, A.N. Sokolov, C. Reese, Z. Bao, "Highly sensitive flexible pressure sensors with microstructured rubber dielectric layers", *Nature Materials*, vol. 9, 2010, PP. 859-864.
- [8] DH Kim, J. Viventi, JJ Amsden, J. Xiao, L. Vigeland, YS Kim, JA Blanco, B. Panilaitis, ES Frechette, D. Contreras, DL Kaplan, FG. Omenetto, Y. Huang, K.C Hwang, M.R. Zakin, B. Litt, J.A. Rogers, "Dissolvable films of silk fibroin for ultrathin conformal bio-integrated electronics", *Nature Materials*, vol. 9, 2010 pp. 511-517.
- [9] I. Minev, D. Chew, E. Delivopoulos, J. Fawcett, S.P. Lacour, "An elastomer microelectrode array for recording afferent nerve activity in an anesthetized rat", 2011, submitted.
- [10] J. FitzGerald, S.P. Lacour, S. McMahon, J. Fawcett, "Microchannel electrodes for recording and stimulation: in vitro evaluation", *IEEE Trans. on Biomed Eng.*, vol. 56, 2009, pp. 1524-1534.
- [11] S. P. Lacour, J. FitzGerald, N. Lago, E. Tarte, S. McMahon, J. Fawcett, "Long micro-channel electrode arrays: a novel type of regenerative peripheral nerve interface," *IEEE Trans. on Neural Systems and Rehabilitation Engineering*, vol. 17, 2009, pp. 454-460.
- [12] D. P. J. Cotton, A. Popel, I.M. Graz, S.P. Lacour, "Photopatterning the mechanical properties of polydimethylsiloxane films," *Journal of Applied Physics*, vol. 109, 2011, p. 120103.
- [13] I.M. Graz, D.P.J. Cotton, A. Robinson, S.P. Lacour, "Silicone substrate with in situ strain relief for stretchable thin-film transistors", *Appl. Phys. Lett.* vol. 98, 2011, pp. 124101-1 – 124101-3.
- [14] I. Graz, M. Kaltenbrunner, C. Keplinger, R. Schwödiauer, S. Bauer, S.P. Lacour, S. Wagner, "Flexible ferroelectret field-effect transistor for large-area sensor skins and microphones," *Applied Physics Letters*, vol. 89, 2006, pp. 073501-1 - 073501-3